PERGAMON

Available online at www.sciencedirect.com

SCIENCE DIRECT®

Corrosion Science 45 (2003) 2819–2835

CORROSION SCIENCE

www.elsevier.com/locate/corsci

Corrosion resistance of HVOF sprayed HastelloyC nickel base alloy in seawater

Jin Kawakita *, Seiji Kuroda, Takeshi Fukushima, Toshiaki Kodama

National Institute for Materials Science, 1-2-1, Sengen, Tsukuba-shi, Ibaraki 305-0047, Japan

Received 28 August 2002; accepted 24 March 2003

Abstract

The nickel base alloy, HastelloyC, deposited by HVOF thermal spraying, was investigated to ascertain the characteristics as a protective coating for the structural steels under the marine environment. Its corrosion resistance was evaluated in addition to its physical and its chemical properties. The HastelloyC deposit with higher impermeability had a comparatively higher corrosion resistance in artificial seawater. It possessed a nature of general corrosion because of its contamination by oxidation of flying particles during the spray process. In the case of the porous deposit, a reaction similar to the crevice corrosion took place on pores between its sprayed particles.

Keywords: Metal coatings (A); EIS (B); Polarization (B)

1. Introduction

In the Ultra Steels Research (STX-21) Project, the thermal spraying was suggested as a coating method alternative to cladding and as a field-mending method of the damaged clad steel around the tidal and the splash zones under the marine environment. Since 1997 the high velocity oxy-fuel (HVOF) spraying has been investigated [1–3], because this technique is able to make a denser and less-oxidized coating, compared with other method such as the plasma spraying [4]. Furthermore, this spraying system enables metals and alloys with the melting point up to about 2000 °C

* Corresponding author. Tel.: +81-29-859-2445; fax: +81-29-859-2401.
E-mail address: kawakita.jin@nims.go.jp (J. Kawakita).

0010-938X/$ - see front matter © 2003 Elsevier Ltd. All rights reserved.
doi:10.1016/S0010-938X(03)00105-7

to be deposited on the target substrate. These features are suitable for an application to the corrosion resistant coating.

So far, several HVOF spray coatings have been subjected to the corrosion test in seawater. In addition to the cermets [5–7], the anti-corrosion alloys [8–10] were adopted as the coating materials. These studies reported that the HVOF method was superior to other spraying techniques in order to make the coatings with a higher protective performance.

For the protective coatings composed of the corrosion resistant materials, impermeability is primarily essential. If such coatings have even a small amount of pores connecting to the substrate, seawater may permeate them and reach the interface between the coating and the substrate. When the conductive solution meets together the contact part of different kinds of conductive material, the galvanic cell, what is called, is formed. A combination of the electrochemically noble coating and the less-noble substrate accelerates corrosion of the substrate, compared to the free substrate with the same surface area. Secondarily, the coatings require the considerably high corrosion resistance in order to exert the protective performance for the long-term service under the severe marine environment.

In order to evaluate the corrosion resistance of HVOF sprayed coatings themselves, we have been spraying a corrosion resistant alloy onto the substrate of the same materials and carrying out various electrochemical tests. This method could ignore corrosion of the substrate by formation of the galvanic couple, as cited above. In our previous study, the deposits of 316L stainless steel by HVOF spraying had a poor corrosion resistance in artificial seawater [3]. This is because SUS316L is one of the materials, which are not strongly resistant to the crevice corrosion in the presence of chloride ion, and because pores or voids were remained between the sprayed particles of the deposits, especially in the external layer near the surface. Therefore, a reaction similar to the crevice corrosion took place on such pores or voids.

In this paper, a nickel base alloy, HastelloyC, was selected as the spray material. This material is known to have a high resistance equivalent to titanium against the crevice corrosion under the marine environment. HastelloyC was deposited onto the bulk plate of HastelloyC276 by the HVOF spray technique. HastelloyC276 has lower contents of both carbon and silicon than HastelloyC. The impermeability of the HastelloyC deposits and their cleanliness were evaluated with respect to porosity and chemical composition, respectively. In addition, their corrosion resistance in artificial seawater was studied using the electrochemical measurements and the microscopic observations.

2. Experimental

2.1. Specimen preparation

The HVOF spraying of HastelloyC was carried out with the TAFA apparatus (JP-5000). This spray process was described in detail in the previous paper [3]. The primary spray conditions were listed in Table 1. The powder of HastelloyC (TAFA

Table 1
Spray conditions

	HP	SP	LP
Fuel flow rate ($dm^3\,min^{-1}$)	0.47	0.38	0.25
Oxygen flow rate ($dm^3\,min^{-1}$)	1080	860	570
Combustion pressure (MPa)	0.86	0.68	0.43
Fuel/oxygen ratio		0.82[a]	
Barrel length (mm)		102	
Powder feed rate ($g\,min^{-1}$)		60	
Torch velocity ($mm\,s^{-1}$)		700	
Spray distance (mm)		380	
Powder feed gas		Nitrogen (N_2)	
Film thickness (μm)		400	

[a] 1.0 corresponds to stoichiometric mixture ratio.

1286F) was 25–53 μm in size and had the following chemical composition: Ni bal, Mo 16.95, Cr 16.57, Fe 6.2, W 4.5, Mn 0.72, Co 0.31, Si 0.73 wt.%. The substrate was the HastelloyC276 bulk plate with a dimension of $2t \times 50 \times 100$ mm. It was blasted with alumina grit and was degreased by ultrasoniciation in acetone. The varied spray parameter in this study was the combustion pressure to prepare three kinds of sprayed coatings. One coating was prepared under the standard condition recommended by the manufacturer, which was termed as SP. The others were prepared under the higher and the lower combustion pressures than SP, which were termed as HP and LP, respectively.

2.2. Characterization

The crystalline phases of the HVOF sprayed deposits were characterized by the X-ray diffraction measurement using the Rigaku apparatus (RINT 2000) with the CuKα radiation.

The oxygen content of the deposits was obtained by the inert-gas fusion method. Its open-porosity was determined by mercury intrusion porosimetry (Micromeritics Autopore II 9220).

The corrosion resistance of the specimen was evaluated by the electrochemical methods with the three-electrode system using both the polarization and the alternating current (AC) impedance measurements. The detailed procedure was described elsewhere [3]. The sample electrode was prepared as follows: (1) the coated specimen was cut into pieces in a size of 2.5 cm^2 and was cleaned ultrasonically in acetone and ion-exchanged water, repeatedly, (2) the stainless lead was connected to the back surface of the substrate plate and (3) the sprayed area of 2 cm^2 was left exposed and the rest of the specimen surface was insulated with silicone resin. The reference electrode was the Ag/AgCl electrode in the saturated KCl solution. The electrolyte was artificial seawater of pH 8.3 at 27 °C. The salt bridge of agar containing KCl was used in addition to the reservoir of artificial seawater to avoid mixing the artificial seawater and the KCl solution. From the polarization measurement, the

potential–current curve was obtained by measuring the current value when the electrode potential of the sample was scanned at the rate of 10 $mV\,s^{-1}$ using a potentiostat with a function generator (Hokuto Denko HAB-151). The sample electrode was immersed in the electrolyte for 24 h to reach the steady state. In this case, the counter-electrode was a platinum plate with a dimension of $0.2t \times 100 \times 100$ mm, and continuous nitrogen bubbling was carried out for de-aeration of the electrolyte.

The polarization resistance of the sample was obtained by the impedance measurement. The AC was applied to the sample electrode at the corrosion potential with amplitude of ± 10 mV. The polarization resistance was determined by subtracting one impedance value at the frequency of 10 kHz from another at 100 mHz with the corrosion monitor (Riken Denshi Model CT-5). In this measurement, the same type of sample electrodes were used for both the working and the counter-electrodes, and continuous air bubbling was carried out for aeration of the electrolyte. The polarization resistance was monitored every 10 min for 3 days in addition to the corrosion potential. For comparison, a bulk plate of HastelloyC276 was used. It was blasted because of the increase in actual surface area.

The surface and the cross section of the specimens were examined by the visual observation, by the optical microscope (Olympus, BX60M), and by the scanning electron microscope (SEM, JEOL JSM-5400). The cross section of the specimen was prepared by embedding the specimen into the epoxy resin, part of which was removed by the abrading and polishing treatments. The chemical composition of the microscopic area of the specimen surface was analyzed by the energy dispersive X-ray spectrometer (EDS, JEOL JED-2140).

3. Results and discussion

3.1. Physical and chemical properties of HVOF sprayed HastelloyC

As the combustion pressure increased, the open-porosity of the HastelloyC deposits by HVOF spraying decreased, as shown in Fig. 1. Over 0.68 MPa, the open-porosity of the deposits reached 0 vol%, which was under the limit of detection by the mercury intrusion porosimetry. In the visual observation, the surface of the sprayed deposits seemed dull and rough, regardless of the spray condition. In the microscopic view, however, there was an obvious difference in the surface state among three types of deposits, as shown in Fig. 2. Almost the entire surface of the LP deposit seemed to be composed of numerous spherical particles. As the combustion pressure increased, the number of the spherical particles decreased whereas the part like a sandy area increased. The cross sectional view of the coating revealed the accumulating state of component particles in the sprayed deposits, as shown in Fig. 3. The LP deposit had small voids between the flattened particles. This void behaved as a small pore in the deposit. Such voids seemed to become small in the SP coating and could not be observed in the HP coating. This phenomenon was due to filling-up of the voids by the fine particles. According to our report, the combustion

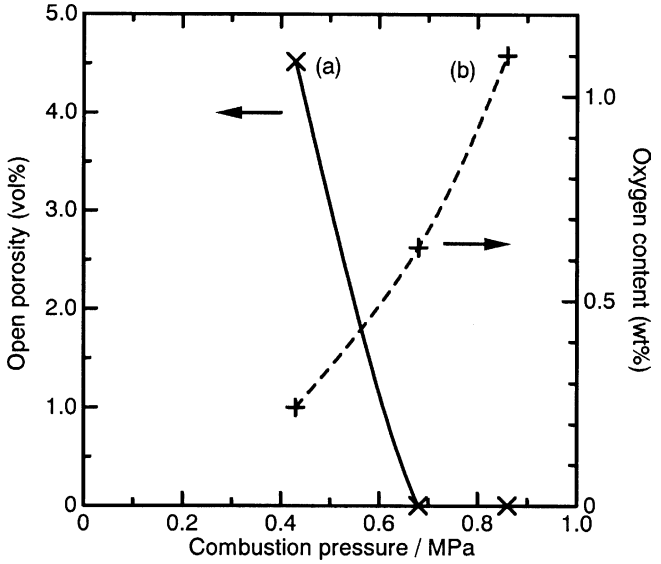

Fig. 1. Relation between combustion pressure and (a) open-porosity and (b) oxygen content of HVOF sprayed HastelloyC deposit.

pressure was related to the flight speed of the sprayed particle as well as its temperature [11]. At the higher combustion pressure, the plastic deformability of the sprayed particles upon impinging to the substrate became higher. Moreover, the fraction of the melted and the softened particles during flying also became larger. As a result, the flattened and fine particles increased, leading to make the closely packed structure.

As the combustion pressure increased, the oxygen content of the HastelloyC deposits increased, as seen in Fig. 1. This was due to the increase in temperature of the spray particle during flying with the increase in combustion pressure, as cited above. Except for oxygen, the sprayed deposits had almost the same content of elements as the supply powder, regardless of the spray condition. At comparatively high oxygen content, some kinds of oxide are expected to be contained in the deposits. No obvious diffraction lines ascribed to oxides, however, appeared in the XRD patterns of the deposits prepared under the LP and the SP conditions, as shown in Fig. 4. Only weak lines implying the presence of the chromium oxide Cr_2O_3 were observed even as for the HP deposit, as marked by arrows in the pattern. All the peaks of the deposits kept the same 2θ in position as those of the supplying powder. Accordingly, the greater part of the sprayed particles kept the f.c.c. phase upon the spray process. The result of transmission electron microscopic (TEM) analysis, however, revealed that some sprayed particles were covered with oxides containing Cr_2O_3, $NiCr_2O_4$, $FeCr_2O_4$. In the cross sectional image of the HP deposit, gray borders were observed surrounding the sprayed particles. Such borders might be due to the existence of the oxide.

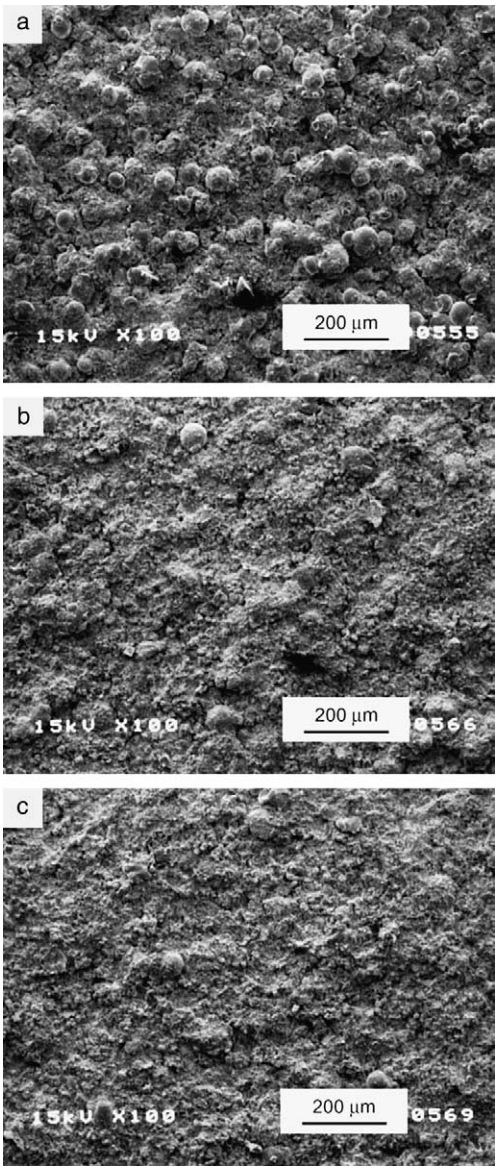

Fig. 2. SEM images of surface of HastelloyC deposits by HVOF spraying under (a) LP, (b) SP and (c) HP conditions.

In addition, all the diffraction lines of the deposits attributed to HastelloyC were less sharper than those of the supplying powder, as compared in Fig. 4. This phenomenon was explained by the deduction that the crystal grain of the deposits decreased in size and became distorted, compared to that of the supplying powder.

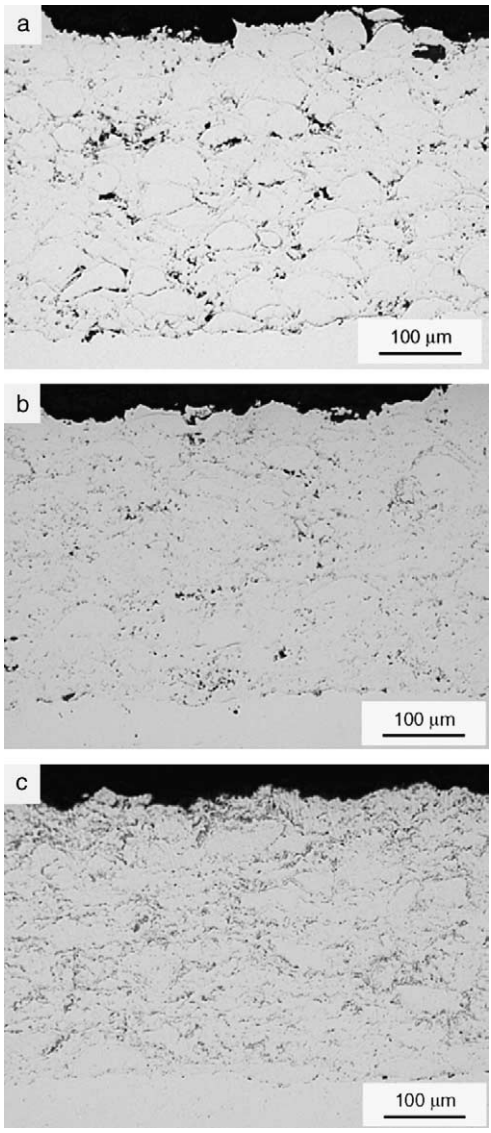

Fig. 3. Optical microscopic images of cross section of HastelloyC deposits on SS400 substrate by HVOF spraying under (a) LP, (b) SP and (c) HP conditions.

3.2. Corrosion resistance of HVOF sprayed HastelloyC

The polarization curves brought about some information about the corrosion resistance of HVOF sprayed deposits under the seawater environment. As seen in Fig. 5, the shape of the curves of the HastelloyC deposits possessed general features

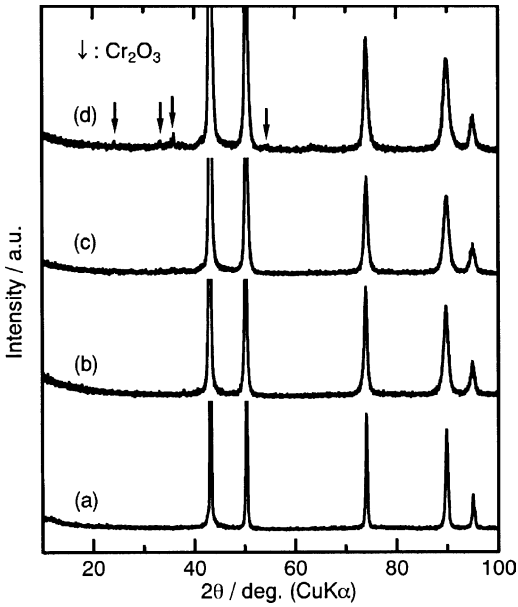

Fig. 4. XRD patterns of (a) supply powder, and deposits of HastelloyC by HVOF spraying under (b) LP, (c) SP and (d) HP conditions.

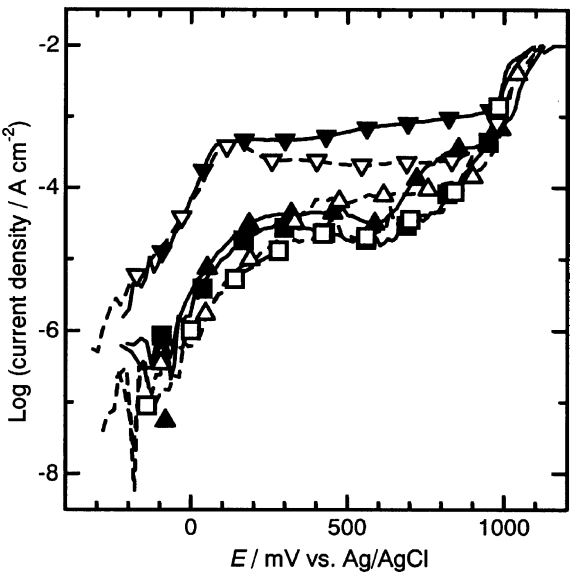

Fig. 5. Anodic polarization curves of HVOF sprayed HastelloyC deposits in de-aerated artificial seawater at 27 °C, ▲: HP (as-sprayed), △: HP (polished), ■: SP (as-sprayed), □: SP (polished), ▼: LP (as-sprayed) and ▽: LP (polished). Scan rate is 10 mV s^{-1}.

of the anti-corrosion metal such as titanium. The anodic current of all the samples increased rapidly with electrode potential in the initial stage of scanning, and thereafter its increasing gradient became small. In the latter region, some samples decreased in anodic current with potential. It is natural that this phenomenon corresponded to formation of oxide or hydroxide on the sample surface. In fact, the surface of most samples became greenish brown after the polarization test, and reaction products appeared on the sample surface, as seen in Fig. 6. Passing through the potential region of stable current, the anodic current of the samples increased rapidly again. Taking account of the comparatively high potential, the reaction in this region corresponded not to pitting corrosion but to oxygen evolution. Even between the as-sprayed and the polished samples under the same spray condition, the difference of anodic current at a certain potential could not be explained simply by their actual surface areas. This difference was presumably due to contribution of a meta-stable oxide formed around the particle surface during the spray process.

As seen in Fig. 5, the LP sample had a considerably larger anodic current than the SP and the HP samples in most of the regions except for oxygen evolution. Fig. 6 shows that the reaction products of the LP sample were observed locally on the surface, in particular between the sprayed particles, while the whole surface of the SP and the HP samples was covered with the reaction products. In the magnified image of the LP surface, some areas were covered with the cracked reaction products while others seemed to remain flat, as seen in Fig. 7a. The microscopic elemental analysis of the LP surface resulted in the considerable difference in chemical composition between the cracked and the flat areas, as listed in Table 2. This could be explained by the relation between the thickness of the reaction products and the penetration depth of the probe electron. The flat area might be covered with thinner reaction products than the cracked area. Accordingly, the high anodic current of the LP sample could be explained by the following reaction mechanism. The LP deposit had a large amount of pores, some of which were connected to each other whereas open-porosity of the SP and the HP deposits was under the limit of detection. In the inner part of such pores, pH of the permeating solution became lower as the anodic reaction proceeded, and the surrounding spray particles there were subject to damage by the corrosion reaction. As a result, the corrosion rate of the LP sample became different at the local sites of its surface, depending on the degree of packing of the sprayed particles.

There remained some round-shape borders on the SP surface while the HP surface seemed to be covered with the reaction product uniformly, as shown in Fig. 6b and c. The former phenomenon was due to the coexistence of the melted and the non-melted particles under the spray condition of SP, as cited above. In the magnified view, such reaction product of the SP and the HP deposits existed on the surface in the cracked state, as shown in Fig. 7b and c. The border between a non-melted particle and surrounding melted areas can be observed on the SP surface, as marked by the arrows. The microscopic elemental analysis of the sample surface revealed the remarkable increase in oxygen content of the reaction product and the change in relative abundance ratio of metal components, as listed in Table 2. The chromium

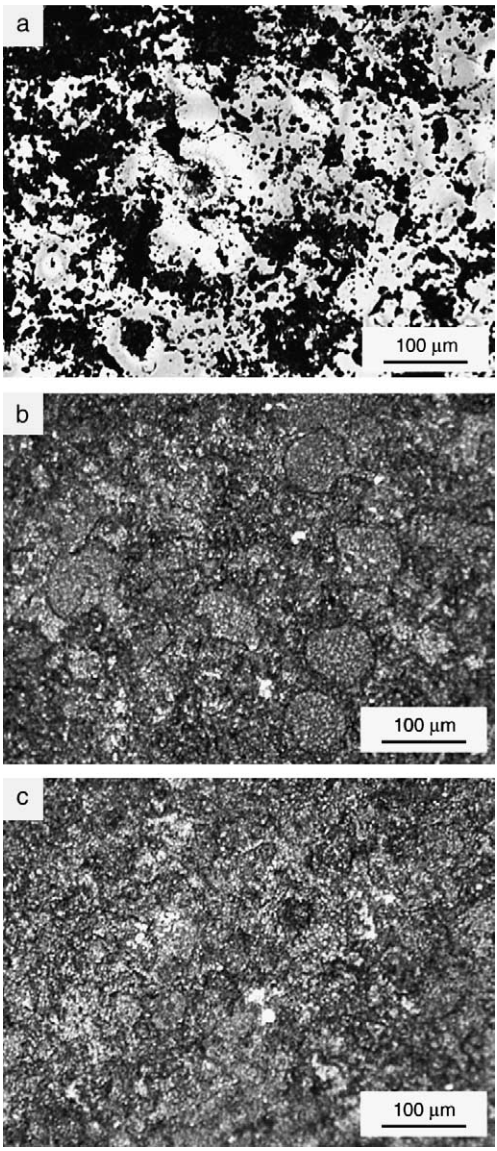

Fig. 6. Optical microscopic images of surface of HVOF sprayed HastelloyC deposits with polishing treatment after anodic polarization measurement: (a) LP, (b) SP and (c) HP.

and the iron elements increased while the nickel and the molybdenum elements decreased. These results brought about the deduction about the reaction mechanism of the HastelloyC deposits during the anodic polarization, as follows: (1) the nickel element was dissolved and (2) the oxide or the hydroxide, mainly composed of iron and chromium, was formed. These results were caused by not retaining the ideal

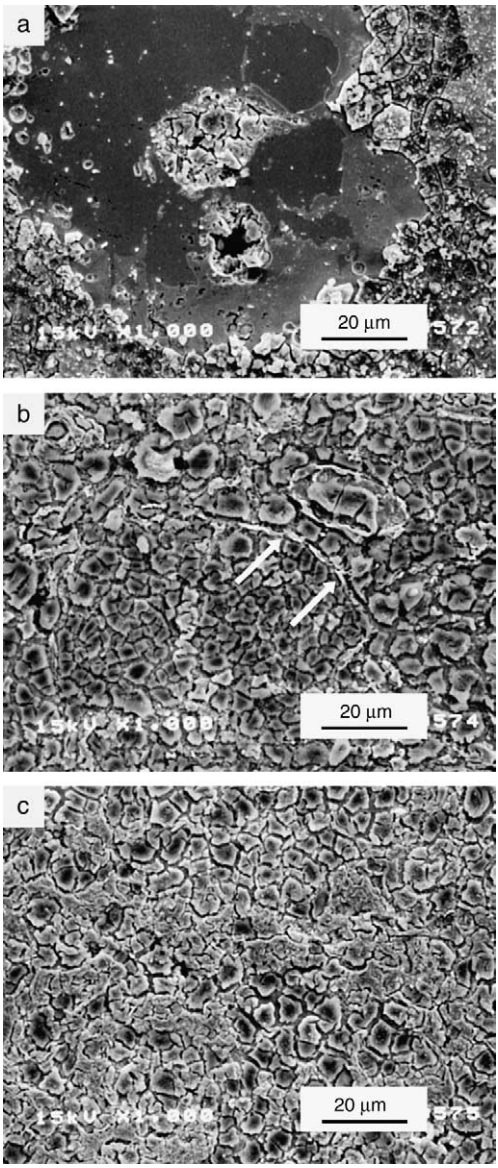

Fig. 7. SEM images of surface of HVOF sprayed HastelloyC deposits with polishing treatment after anodic polarization measurement: (a) LP, (b) SP and (c) HP.

composition of HastelloyC, especially near the surface because the spray particles were oxidized during the flight in the spray process.

The static corrosion resistance of HVOF sprayed deposits in seawater was estimated by both the corrosion potential and the polarization resistance under the

Table 2
Chemical composition of surface after polarization test

		Ni	Cr	Mo	Fe	O
Cracked area	LP	3.83	10.53	9.86	9.18	66.59
	SP	5.09	12.05	3.53	14.00	65.34
	HP	10.00	12.04	4.57	11.55	61.85
Flat area	LP	48.16	17.01	11.57	7.04	16.22

simple immersion condition. Without the polishing treatment, i.e. under the as-sprayed state, the LP deposit had a lower potential than the HP and the SP ones for 3 days of immersion, as shown in Fig. 8. This was explained by the reaction similar to the crevice corrosion in the inner part of connecting pores between spray particles, as cited above. As shown in Figs. 9 and 10, the spot rusts were observed on the surface of the LP deposit after immersion while the HP and the SP deposits had no such visible rusts. With the polishing treatment, the HP and SP deposits increased gradually in the corrosion potential with the time of immersion (see Fig. 8). This phenomenon suggested the formation of oxide on the polished surface. This oxide, however, might be extremely thin and could not be detected by the microscopic observation as well as the visible observation, as shown in Figs. 9 and 10, respectively. The polarization resistance, R_p, is one of the criterions for comparison of the

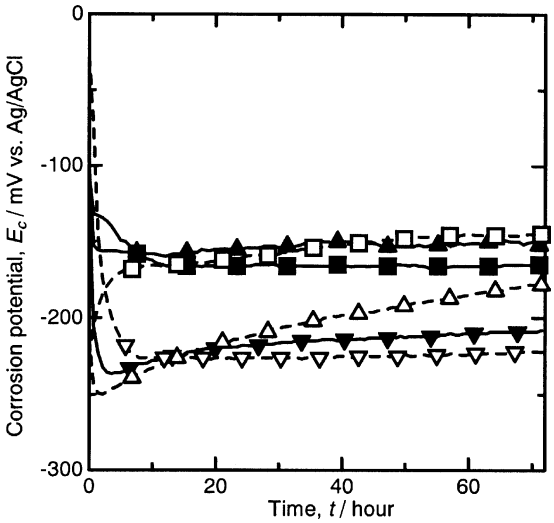

Fig. 8. Change in corrosion potential of HVOF sprayed HastelloyC deposits with time in aerated artificial seawater at 27 °C, ▲: HP (as-sprayed), △: HP (polished), ■: SP (as-sprayed), □: SP (polished), ▼: LP (as-sprayed) and ▽: LP (polished).

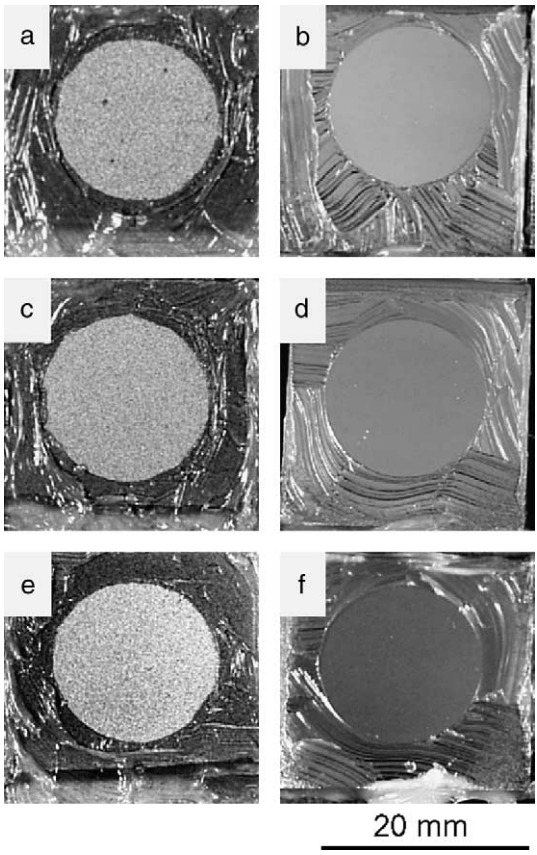

Fig. 9. Photographs of HVOF sprayed HastelloyC deposits after immersion for 3 days: (a) LP (as-sprayed), (b) LP (polished), (c) SP (as-sprayed), (d) SP (polished), (e) HP (as-sprayed) and (f) HP (polished).

materials in terms of the corrosion resistance. The difference in resistance between the as-sprayed and the polished deposits corresponded to the difference in the actual surface area. Regardless of the surface treatment, the LP deposits had a lower resistance than the HP and the SP ones, as shown in Fig. 11. This was caused by the different kinds of corrosion reaction. The LP deposit was subject to the crevice corrosion while the oxide was formed on the HP and SP surfaces. The corrosion products were observed locally on the LP surface, as Figs. 9a and 10a. In the initial stage of immersion, the LP deposits decreased rapidly in resistance with time and increased gradually, indicating the permeation of the test solution into pores of the deposits, followed by the filling-up of such pores by the corrosion products. The SEM images revealed that the corrosion product grew in such pore, which was finally closed with the corrosion products, as shown in Fig. 12. A gradual increase of the

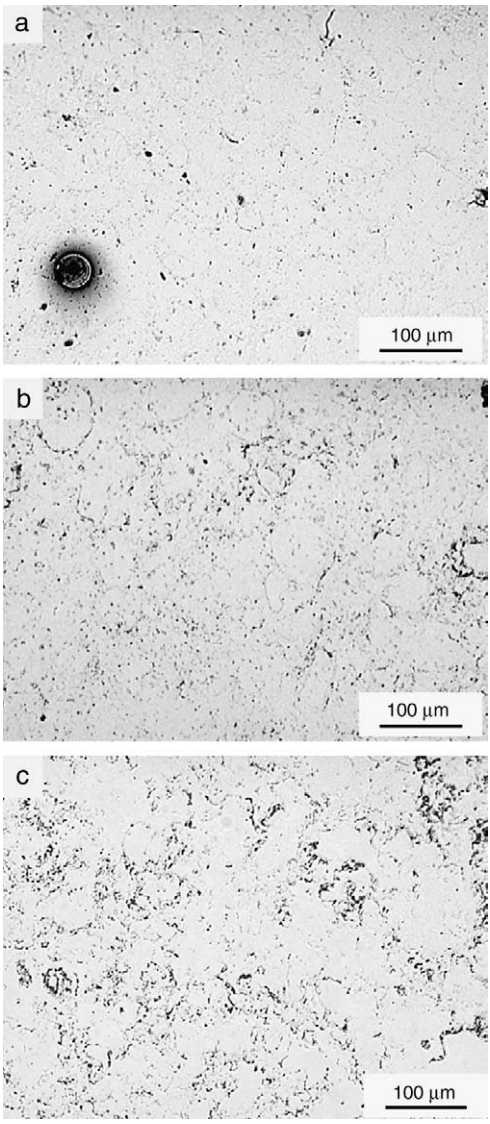

Fig. 10. Optical microscopic images of surface for HVOF sprayed HastelloyC deposits with polishing treatment after immersion for 3 days: (a) LP, (b) SP and (c) HP.

polarization resistance was observed for the HP and the SP deposits in the initial stage of immersion (see Fig. 11). This phenomenon suggested the uniform formation of thin and less-conductive oxide on the surface. The HP and SP deposits possessed the high corrosion resistance, resulted from comparatively high polarization resistance around $10^5\ \Omega\,cm^2$. From this value, the corrosion rate, R_c, was estimated

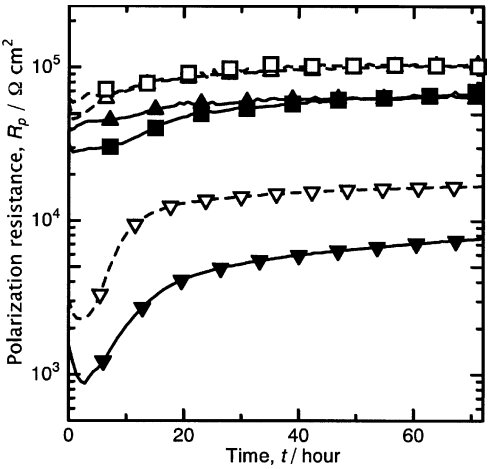

Fig. 11. Change in polarization resistance of HVOF sprayed HastelloyC deposits with time in aerated artificial seawater at 27 °C, ▲: HP (as-sprayed), △: HP (polished), ■: SP (as-sprayed), □: SP (polished), ▼: LP (as-sprayed) and ▽: LP (polished).

roughly to be in the order of 10 μm year^{-1}, assuming that R_c is connected to R_p by the following equation [12]:

$$R_c = K \times R_p^{-1} \tag{1}$$

In this equation, K is a conversion coefficient of 10^2 Ω cm^3 year^{-1}, based on both the observed value of $R_p = 10^6$ Ω cm^2 for the HastelloyC276 plate and the literature data of $R_c = 0.001$ mm year^{-1} for HastelloyC [13].

4. Conclusion

The HastelloyC deposits with significantly high impermeability could be obtained by the increase in energy of the flame during HVOF spraying. Their open-porosity could be reduced to 0 vol%, i.e. under the limit of detection by the mercury intrusion porosimetry. As the flame energy increased, however, the cleanliness of the deposits became lower, especially the oxide content increased. This is because the higher flame energy lead to increase in fraction of the melted and the softened particles suitable for making the dense structure and simultaneously to increase in temperature of the flying particles.

The corrosion resistance of the HVOF sprayed HastelloyC deposit was comparatively high under the seawater environment. Its corrosion rate was estimated to be in the order of 10 μm year^{-1} from the result of the electrochemical AC impedance measurement. The primary corrosion reaction of the deposit was uniform formation of the oxide or the hydroxide on its whole surface. When pores existed between the sprayed particles of the deposits, such places were subject to the predominant

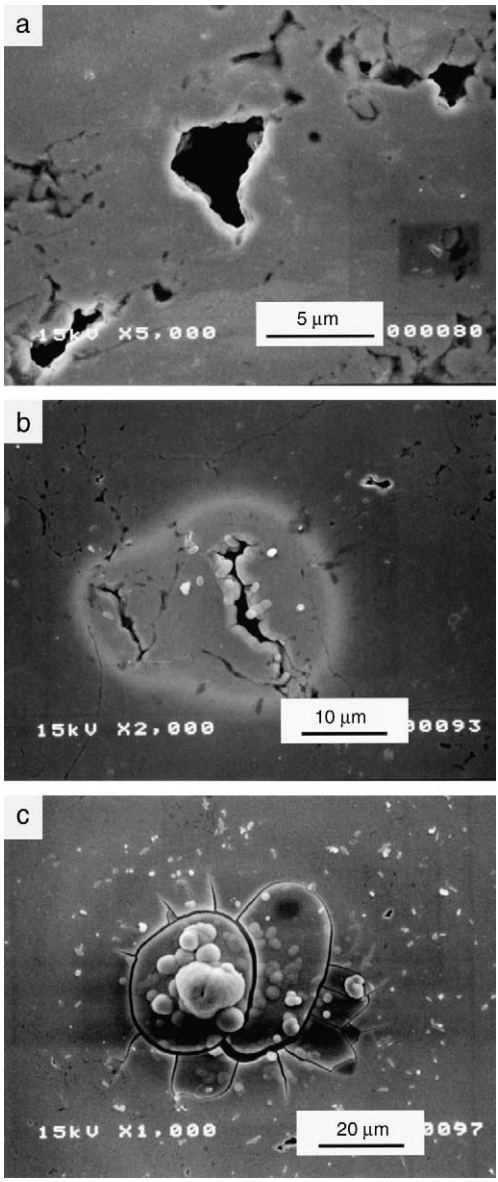

Fig. 12. SEM images of surface of HastelloyC deposit by HVOF spraying under LP condition with polishing treatment (a) before and (b and c) after immersion for 3 days.

corrosion reaction and the corrosion rate there was considerably faster than that in the normal sprayed parts. As the result, the local corrosion seemed to take place there.

In order to improve the corrosion resistance of the HastelloyC coating, it is essential to decrease its contamination by oxidation.

References

[1] S. Kuroda, T. Fukushima, M. Sasaki, T. Kodama, in: Proc. 1st Int. Thermal Spray Conf., Montréal, Québec, Canada, 8–11 May 2000, ASM International, p. 455.
[2] J. Kawakita, T. Fukushima, S. Kuroda, T. Kodama, in: Proc. Int. Thermal Spray Conf., Singapore, 28–30 May 2001, ASM International, p. 1137.
[3] J. Kawakita, T. Fukushima, S. Kuroda, T. Kodama, Corros. Sci. 44 (2002) 2561.
[4] H. Herman, S. Sampath, R. McCune, MRS Bull. (July) (2000) 17.
[5] A. Naville, T. Hodgkiess, Surf. Eng. 12 (1996) 303.
[6] M. Guilemany, J. Fernández, J.M. de Paco, J. Sanchez, Surf. Eng. 14 (1998) 133.
[7] A. Collazo, X.R. Nóvoa, C. Pérez, Electrochim. Acta 44 (1999) 4289.
[8] P. Gu, B. Arsenault, J.J. Beaudoin, J.G. Legoux, B. Harvey, J. Fournier, Cerm. Conc. Res. 28 (1998) 321.
[9] A.J. Sturgeon, D.C. Buxton, in: Proc. 1st Int. Thermal Spray Conf., Montreal, Canada, 8–11 May 2000, ASM International, p. 1011.
[10] D. Harvey, O. Lunder, R. Henriksen, in: Proc. 1st Int. Thermal Spray Conf., Montreal, Canada, 8–11 May 2000, ASM International, p. 991.
[11] H. Yamada, S. Kuroda, T. Fukushima, H. Yumoto, in: Proc. Int. Thermal Spray Conf., Singapore, 28–30 May 2001, ASM International, p. 797.
[12] M. Stern, A.L. Geary, J. Electrochem. Soc. 104 (1957) 56.
[13] V.F. Ritter, Korrosionstabellen Metallischer Werkstoffe, Springer-Verlag, Austria, 1958, translated by H. Nagasaka, M. Midorikawa, Japan UNI Agency, Japan, 1979, p. 294.